Chapter 4 – F-16XL GEOMETRY AND GRIDS

by

Okko J. Boelens, Stefan Görtz, Scott Morton, Willy Fritz, Steve L. Karman Jr., Todd R. Michal and John E. Lamar *(Retired)*

4.1 SUMMARY

The objective of the Cranked-Arrow Wing Aerodynamics Project International (CAWAPI) was to allow a comprehensive validation of Computational Fluid Dynamics methods against the CAWAP flight database. A major part of this work involved the generation of high-quality computational grids. Prior to the grid generation an IGES file containing the air-tight geometry of the F-16XL aircraft was generated by a cooperation of some of the CAWAPI partners. Based on this geometry description both structured and unstructured grids have been generated. The baseline structured (multi-block) grid (and a family of derived grids) has been generated by the National Aerospace Laboratory (NLR). The baseline all-tetrahedral and hybrid unstructured grids were generated at the NASA Langley Research Center and the U.S. Air Force Academy, respectively. To provide more geometrical resolution, additional unstructured grids were generated at EADS-MAS, the UTSimCenter, and Boeing Phantom Works. All the grids generated within the framework of CAWAPI will be discussed.

4.2 INTRODUCTION

The objective of the CAWAPI was to allow a comprehensive validation and evaluation of CFD methods against the CAWAP flight database (see Chapter 3 and [4-1]). Part of the work involved the generation of high-quality computational grids.

In order to allow high-quality grid generation, the available CAD geometry description of the F-16XL aircraft was scrutinized. Issues encountered during this process are discussed in Section 4.3.

At the beginning of the project the task group members recognized the need to use common grids around this complex geometry to eliminate most of the uncertainties related to grid. The original plan was to have two common grids, one structured (multi-block) and one unstructured (tetrahedral). However, whereas all partners using structured CFD methods performed their simulation on a common structured multi-block grid generated at Netherlands National Aerospace Laboratory NLR (see Section 4.4), most partners using unstructured CFD methods have generated their own unstructured grid during the course of the project or have adapted existing grids (see Section 4.5). A section with conclusions completes the chapter.

4.3 GEOMETRY DESCRIPTION

The geometry of the F-16XL aircraft is based on the Full-Scale Development F-16A. It was obtained from this aircraft by stretching the fuselage and adding a cranked-arrow wing, which has a leading-edge sweep angle of 70° inboard and 50° outboard of the crank. An 'S-blend curve' was placed in the leading edge at the juncture of the wing leading edge with the fuselage. During all CAWAP flight tests the aircraft was equipped with an air dam upstream of the actuator pod and wing-tip missiles. The F-16XL aircraft has been described in detail in Chapter 3.

At the beginning of CAWAPI two IGES files of the F-16XL aircraft were available, one from Lockheed-Martin Aeronautics Company and one from NASA Langley. The latter was obtained by measuring the actual aircraft in the NASA hangar, where a numerical surface description (NSD) was obtained through photogrammetric targets. This measurement was performed in the framework of the HSR program (see Chapter 3 and [4-1]). Using both surface descriptions and additional CATIA models for the inlet up to the compressor face and for the nozzle up to the turbine face, an updated IGES file was generated by Lockheed-Martin Aeronautics Company. It should be noted that for the configuration used the control surfaces were not deflected. This IGES file contained a better characterization of the actual aircraft surfaces and the leading edges, but was still not suitable for further grid generation purposes. It was found that the geometry description contained multiple overlaying surfaces. This was corrected at EADS-MAS, where a single set of describing surfaces was generated. The resulting description also included some refinements in the wing leading-edge region to improve future grid generation in this region. It was recognized by the CAWAPI members that this surface description needed some further adjustments to facilitate the generation of a structured grid. The following modifications were applied:

- The gap between the launcher and the missile was closed. Other details of the missile, such as the fins, were unmodified.
- The gap between the nozzle and the trailing-edge flap was closed.
- The environmental control system (ECS) inlet was simplified.
- A step in the longitudinal progression of the nose-boom outer diameter was smoothed out.

These modifications were made at the NASA Langley Research Center. Finally, the modified surface description was checked for water tightness and corrected, where necessary, using the CAD tool ‘CADfix’ [4-16]. The IGES file containing the air tight geometry description (see Figure 4-1) was used for both the structured and unstructured grid generation.

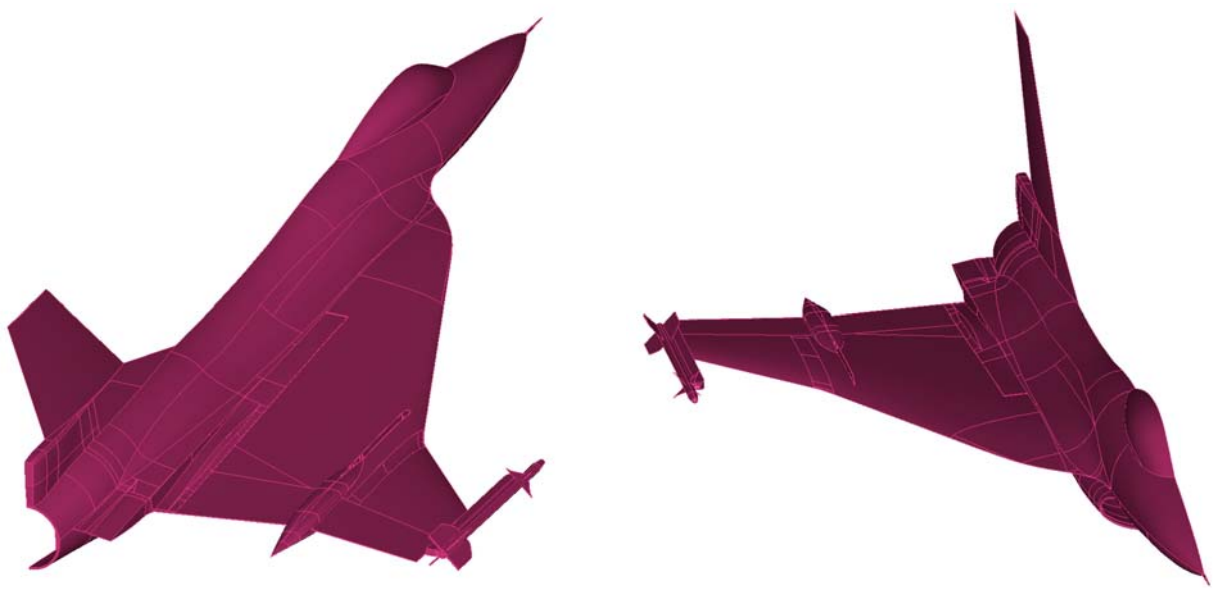

Figure 4-1: CAD Geometry Representation of the F-16XL Aircraft.

4.4 STRUCTURED GRID

4.4.1 Background

During CAWAP a structured grid had been generated at NASA Langley Research Center [4-1]. This grid was based on a prior IGES file and exhibited an average value of y^+ of 82 at flight Reynolds numbers. Simulations on this grid were performed using the 'wall function' option in the turbulence model to compensate for the insufficient grid spacing. It was, therefore, decided that for CAWAPI purposes a new structured grid had to be generated.

The plan, as detailed in [4-10], was for "two members of the CAWAPI – one at the Netherlands National Aerospace Laboratory (NLR) and the other at the U.K. University of Glasgow (UGlasgow) –" to "collaborate in the development of the structured grid for their own use as well as for others. This is a risky endeavor even if the developers are co-located or on the same hall, but certainly more-so if they are in two different countries and having to rely on the Virtual Laboratory (VL) for all grid exchanges. The plan was for the NLR to produce the blocking strategy with implementation and for UGlasgow to adjust the grid spacing, as needed. Alternatively, NLR could produce and test the grid then UGlasgow would perform a second test on the grid before its general release to the facet. In either case, both would use and support the same grid file. For this problem, it turned out that the alternate plan was the one implemented due, in part, to the difficulties experienced with the transfer of large files…from this newly developed VL."

4.4.2 Grid Generation Algorithm

The structured grid has been generated at the Netherlands National Aerospace Laboratory NLR using a Cartesian grid mapping technique. The (semi-automatic) grid generation algorithms are developed at NLR and are part of NLR's ENFLOW flow system [4-2]. Most of these algorithms had become available just before CAWAPI and had only been applied to a clean (no external loads) F-16 configuration. Being the first realistic case to which these tools were applied and bearing in mind that a limited experience with their use existed, it was estimated that six weeks would be needed to generate the complete structured (multi-block) grid.

The Cartesian grid generation technique used by the Netherlands Aerospace Laboratory NLR can be subdivided in the following steps:

1) *Imagine/construct a Cartesian abstraction of the geometry description.* In such an abstraction, the geometry including all details is represented by a set of Cartesian blocks. The abstraction of the half-span full-scale model of the F-16XL used in CAWAPI is shown in Figure 4-2 (a). In this figure, it can be seen that each fin of the wing tip missile for example is represented by a single block. Note furthermore that in this abstraction the engine duct and the nozzle have been closed.
2) *Project the abstraction onto the real geometry description.* The projected abstraction of the half-span full-scale model of the F-16XL is shown Figure 4-2 (b).

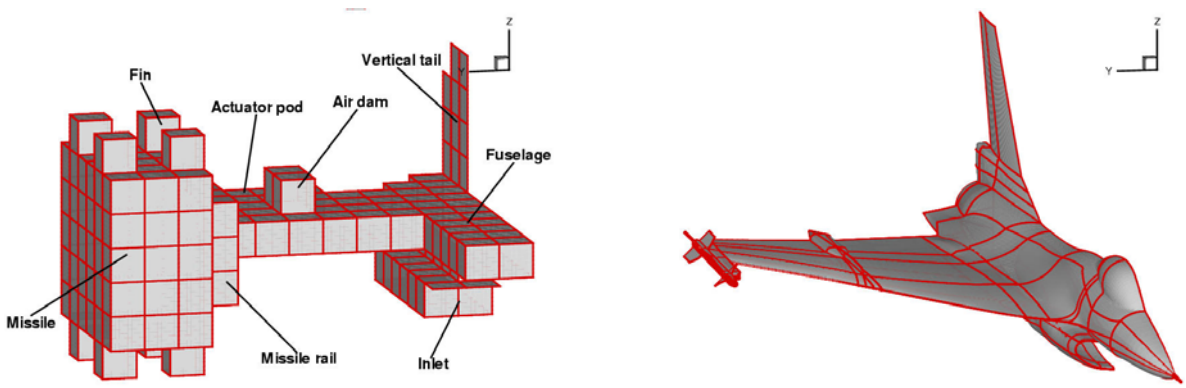

(a) (b)

Figure 4-2: Abstraction of the Surface Geometry (a) and Projected Abstraction (b) for the F-16XL Half-Span Model.

3) *Generate the so-called Navier-Stokes blocks.* This first layer of blocks around the geometry including the engine duct and the nozzle is generated by a simple blow-up technique. The surface patches are translated along the outward normal to the geometry using the corners of the patches as control points. The algorithm used accounts for symmetry planes and only needs the off-set of the blocks as input. The generated layer of blocks has an O-O-type topology. During this step also the blocks to fill up the engine duct and the nozzle are inserted interactively.

4) *Generate the field blocks in the Cartesian space*. The faces of the Navier-Stokes blocks opposite to the geometry combined with the faces at the engine duct inlet and nozzle exit display the same Cartesian structure as the abstraction shown in Figure 4-2 (a). In the Cartesian space the field blocks are generated automatically. As is evident from Figure 4-2 (a), the blocks in the Cartesian space are simple cubical blocks.

5) *Generate the field blocks in the physical space*. The simple cubical blocks in the Cartesian space are automatically mapped to the physical space using a grid deformation technique [4-3]. The algorithm accounts for symmetry planes. Finally, so-called far-field blocks are added to the topology interactively, see Figure 4-3. The far-field boundaries are located several reference wing chords away from the model.

6) *Set the (Euler) grid dimensions*. Each edge is assigned a grid dimension. The minimum number of cells used along an edge is eight, to ensure three levels of multi-grid. In the Navier-Stokes blocks, eight cells were used in the surface normal direction.

7) *Automatically connect the edges.* The grid spacing in the grid is set automatically. For each set of adjoining edges the grid point density is adjusted such that a smooth transition of the grid is obtained. In general, this means that the grid point density of the edge with the larger grid spacing is linked to that of the edge with the smaller grid spacing.

8) *Improve the grid quality by an elliptical smoothing algorithm.* An elliptical smoothing algorithm is applied to the grid. As a result of this algorithm the quality in terms of grid smoothness is improved significantly.

9) *Increase the resolution in the Navier-Stokes blocks*. To provide for sufficient boundary layer resolution the number of grid points in the surface normal direction is increased. In addition a redistribution of the grid points with a specified stretching away from the geometry is applied. The algorithm used accounts for a smooth transition to the grid in the outer blocks.

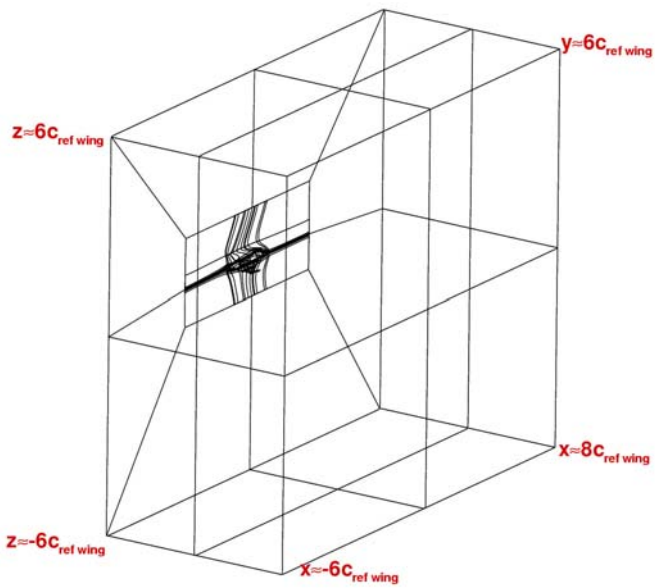

Figure 4-3: Topology on the Geometry, the Symmetry Plane and the Far-Field Boundaries.

Within NLR's ENFLOW CFD system further algorithms exist to:

- Merge blocks within a grid to reduce the total number of blocks.
- Mirror a grid with respect to a symmetry plane to obtain a full-configuration grid from a half-configuration grid.
- Convert the grid from NLR's native ENFLOW format to several other formats, such as Plot3D or CGNS [4-9].

The characteristics of the structured grid obtained using this Cartesian grid mapping technique are described in the next section. Instead of the six weeks estimated prior to the project, the structured grid was generated well within four weeks.

4.4.3 Characteristics of the Grid

During the structured grid generation process the following small modifications to the surface description were made to further facilitate the generation of a structured grid:

- A small 'step' or 'plate' on the wing upper surface was removed.
- The end part of the vertical tail base was slightly rounded off.

The following family of structured grids has been used in CAWAPI:

- The baseline structured grid around the half-span full-scale model of the F-16XL consisting of 1903 blocks, 14,750,720 grid cells and 17,014,119 grid points.
- The above described baseline structured grid with the far-field blocks divided into smaller blocks so that only a one-to-one connection between block faces exists. This version was used by the University of Liverpool.

- The baseline structured grid with a reduced number of blocks. The first merging step was performed at NLR reducing the number of blocks from 1903 to 216. A further small reduction was accomplished at NASA Langley Research Center which yielded a grid with only 200 blocks.
- A structured grid around the full-scale model of the F-16XL consisting of 3806 blocks, 29,501,440 grid cells and 34,028,238 grid points. This grid has been generated by mirroring the baseline structured grid around the half-span full-scale model of the F-16XL with respect to the symmetry plane. This grid has only been used by NLR.

Some details of the baseline structured grid around the half-span full-scale model of the F-16XL are summarized in Table 4-1.

Table 4-1: Details of the Baseline Structured Grid

Number of blocks	1903
Number of boundary layer blocks	367
Number of far-field blocks	20
Number of points in Navier-Stokes blocks in surface normal direction	32
First normal distance from the wall, Δs_1 [m]	6.0×10^{-6} (7.9×10^{-7} $c_{ref\ wing}$)
Viscous grid layer geometric progression parameter, $\Delta s_2/\Delta s_1$	1.1
x_{min}, x_{max}[m]	-45, 60 (-5.97 $c_{ref\ wing}$,7.96 $c_{ref\ wing}$)
y_{min}, y_{max}[m]	0 , 45 (0, 7.96 $c_{ref\ wing}$)
z_{min}, z_{max}[m]	-45, 45 (-5.97 $c_{ref\ wing}$, 5.97 $c_{ref\ wing}$)

The upper surface grid is shown in Figure 4-4. In Figure 4-5, the grid is shown in both a plane approximately normal to the flow direction (FS is constant) and in a plane approximately parallel to the flow direction (BL is constant). Finally, the resulting y^+ distribution over the upper surface is shown in Figure 4-6. From this figure, it is evident that the grid spacing normal to the surface has a desired value of y^+ less then one, except for the regions below the vortical structures.

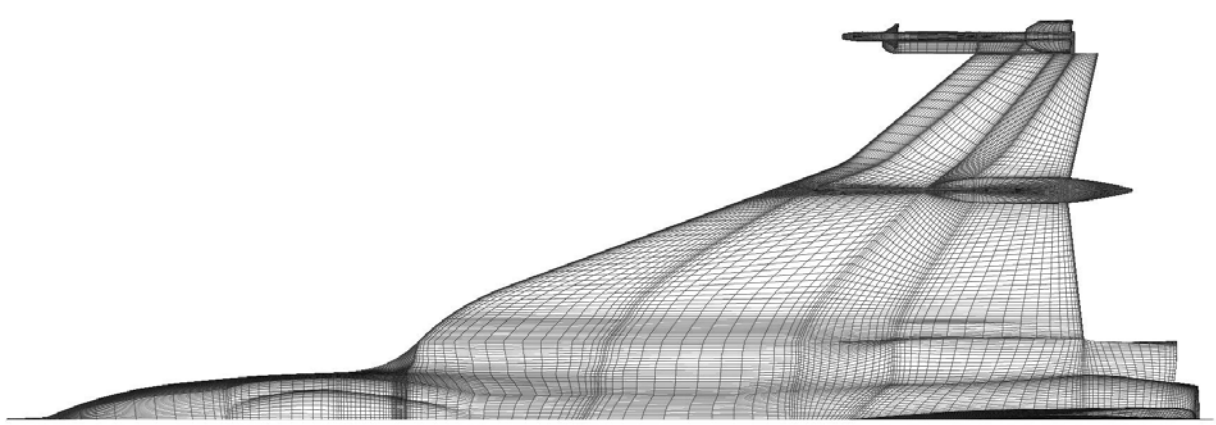

Figure 4-4: Upper Surface Grid for the Structured Grid.

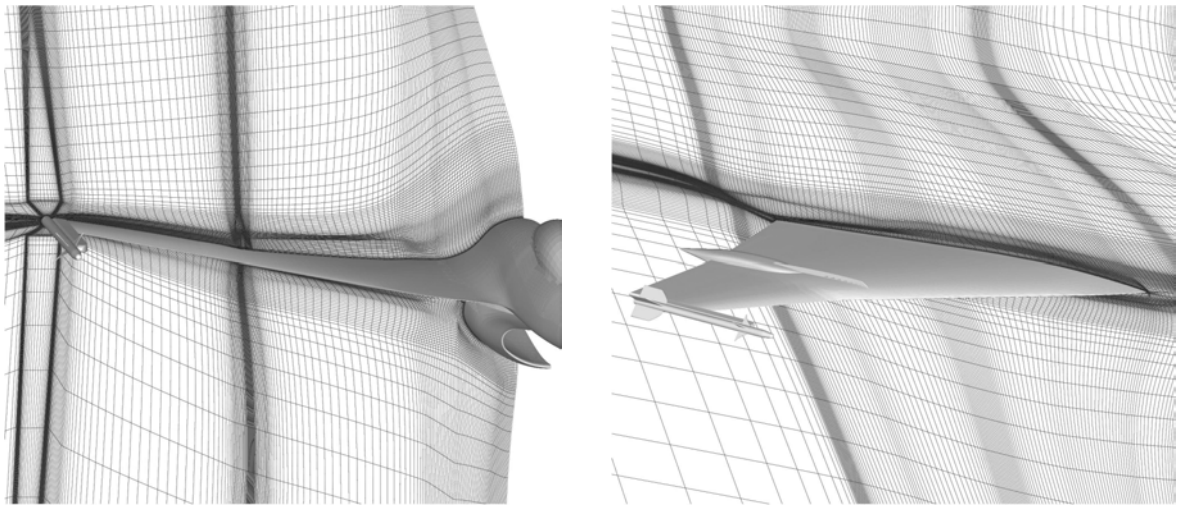

(a) (b)

Figure 4-5: Grid Planes Showing the Grid Density Off the Aircraft Surface in a Plane Approximately Normal to the Flow Direction (FS is constant) (a) and in a Plane Approximately Parallel to the Flow Direction (BL is constant) (b).

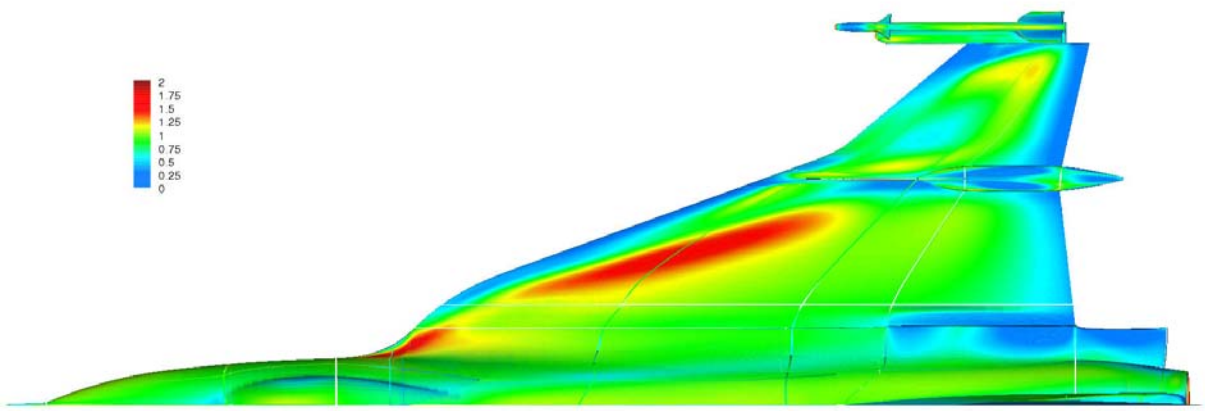

Figure 4-6: Levels of y^+ on the Upper Surface for Flight Condition 19 (TNT k-ω Turbulence Model with Correction for Vortical Flows).

4.5 UNSTRUCTURED GRIDS

4.5.1 Baseline Unstructured Grid

The baseline unstructured 3D all-tetrahedral viscous grid with 2,534,132 nodes, corresponding to 14,802,429 cells, was generated for a half-span full-scale model of the F-16XL-1 (control surfaces not deflected) at the NASA Langley Research Center using the grid generation packages GridTool [4-4] and VGRIDns [4-5].

This grid was converted to a hybrid baseline unstructured grid in Cobalt [4-6] format at the U.S. Air Force Academy using the commercial grid management utility Blacksmith from Cobalt Solutions, LLC. Blacksmith

reduced the cell count to a total of 11,928,103, corresponding to 2,535,842 nodes, by combining highly stretched tetrahedral cells into prismatic cells. The program generated 9 layers of prismatic cells, corresponding to 1,442,394 prisms. The reason the grid had only 9 prismatic layers is that pyramids would be needed as "end caps" for layers that are not complete. Rather than adding another cell type it was decided to accept 9 layers. The transition between the prismatic layers and the tetrahedral grid is very smooth. The surface of the half-span model of the F-16XL is discretized with 160,266 triangular elements. The upper surface grid is shown in Figure 4-7.

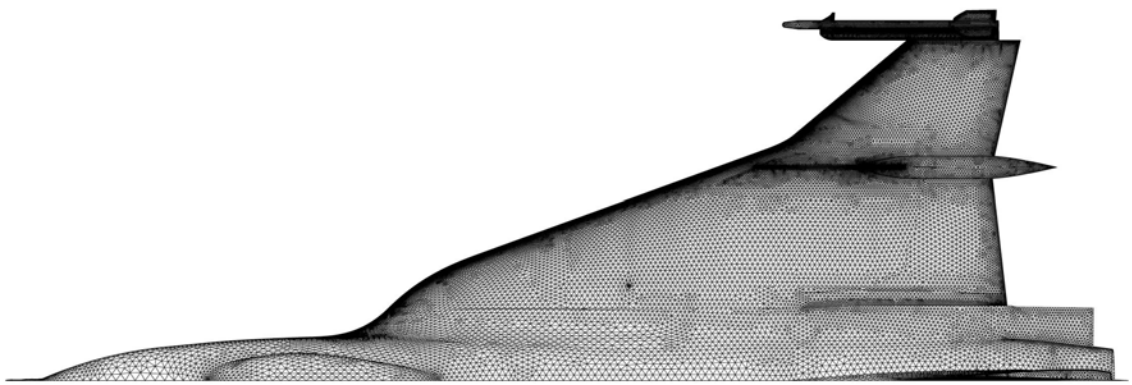

Figure 4-7: Surface Grid of the Hybrid Baseline Unstructured Grid for the F-16XL-1 Half-Span Model (160,226 Faces).

The resolution of the boundary layer requires the grid to be clustered in the direction normal to the surface with the spacing of the first grid point off the wall to be well within the laminar sub-layer of the boundary layer. For turbulent flows, the first point off the wall should exhibit a y^+ value of less than 1.0. Here, the spacing of the first grid point normal to the solid wall is 5.0 x 10^{-6} m (6.6 x 10^{-6} c). Away from the wall, the spacing increases by a ratio $\Delta s_2/\Delta s_1$ of 1.2. The resulting y^+ distribution over the upper surface of the aircraft model is shown for flight condition 19 in Figure 4-8. It can be seen that the grid spacing normal to the surface led to an average value of y^+ of less than one and a maximum y^+ of about two under the primary wing vortex, demonstrating that the grid is fine enough at the wall boundaries.

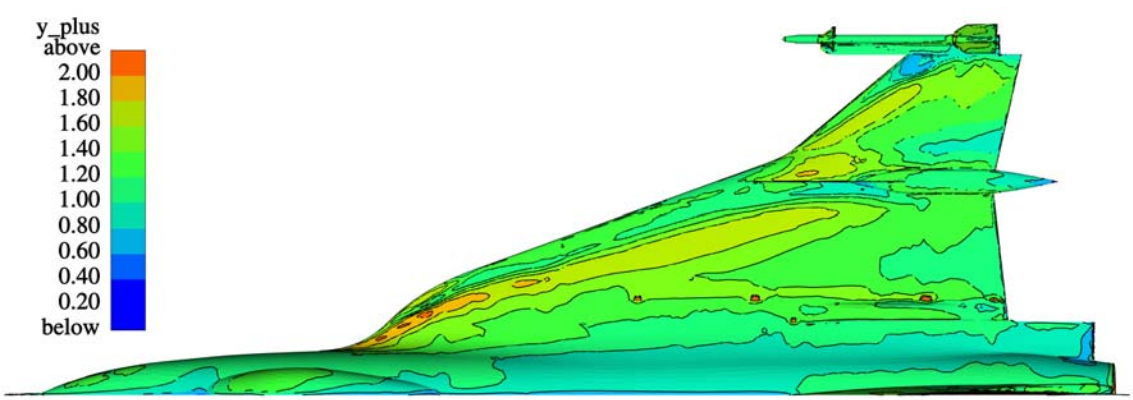

Figure 4-8: Levels of y^+ on the Upper Surface for the Hybrid Baseline Unstructured Grid for Flight Condition 19 (EARSM).

The engine duct is meshed all the way to the inlet duct exit plane. The nozzle is meshed from the engine mixing plane, see Figure 4-9. The grid density off the aircraft surface is shown in Figure 4-10, which depicts a wrinkly cutting plane through the grid at FS496 (fuselage station on airplane in inches, positive aft), close to the trailing edge.

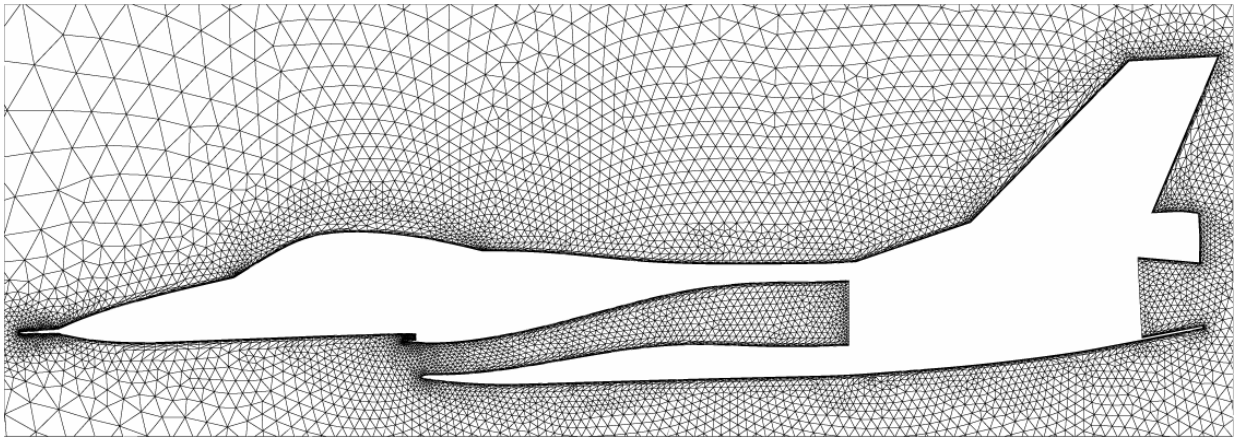

Figure 4-9: Symmetry Plane of the Hybrid Baseline Unstructured Grid Showing the Meshed Inlet Duct and Nozzle.

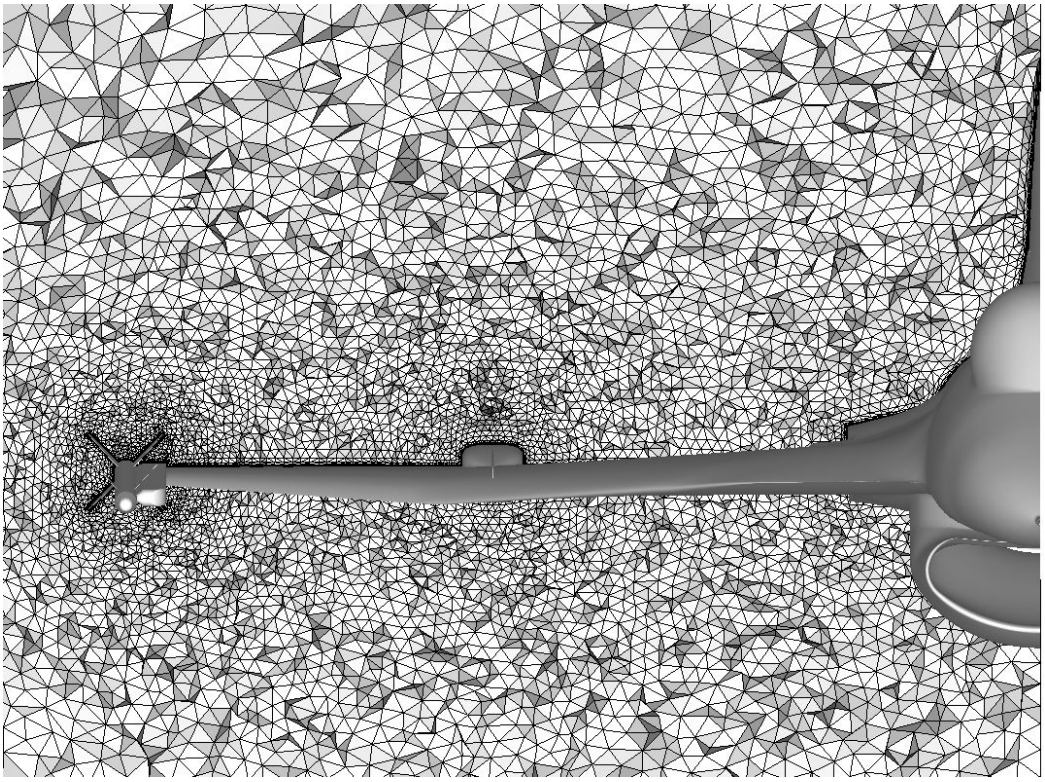

Figure 4-10: Wrinkly Cutting Plane at FS496 Showing the Grid Density Off the Aircraft Surface Close to the Trailing Edge of the Wing.

Next, the group at KTH converted the hybrid grid from Cobalt format to the "Flexible Format Architecture" (FFA) [4-7], the native format of the Swedish CFD code Edge [4-8]. In this conversion step, all grid dimensions were converted from inches to meters.

Finally, KTH researchers converted the FFA-format grid to the CFD General Notation System (CGNS) [4-9] library version 2.3. The resulting CGNS file was uploaded to the Virtual Laboratory (VL) [4-10] at NASA Langley Research Center to be used by other researchers in CAWAPI.

4.5.2 Other Unstructured Grids

4.5.2.1 EADS-MAS

At EADS-MAS the adaptation technique, which is included in the DLR-TAU code [4-11], was used for the CAWAPI CFD simulations (see also Chapter 8). Starting point was a so called initial grid, which subsequently is adapted four times during the flow simulations. This starting grid was a hybrid grid with 10,496,522 nodes in total for the half-span full-scale model of the F-16XL. It has a prismatic layer of 15.6 million prisms in the near wall region and 13.5 million tetrahedra in the outer region. The thickness of the first prismatic layer is 4.0e-06 m and a geometric progression parameter $\Delta s_2/\Delta s_1$ of 1.3 is used for the other 29 viscous layers. In critical regions the prismatic layers are chopped and transition elements such as pyramids and tetrahedra are created. The surface of the aircraft is resolved by 749,742 triangles.

This initial grid was generated using the CentaurSoft grid generator [4-12], which enables the generation of hybrid grids with minimal user interaction. Starting from the air tight geometry description, the grid generation process is split up into surface triangulation, prismatic grid generation and tetrahedral grid generation. Point clustering is achieved by automatic clustering based on geometric features and by user-controlled clustering placing so called sources. This user controlled clustering has been used for a rough adaptation of the grid to the expected vortical flow structure. The surface triangulation works patch-oriented, which results in a not always needed high resolution of all small surface patches. (The geometry definition of the F-16XL contains several such mini-patches). As the adaptation algorithm of the TAU code uses the surface grid as geometry base, the surface triangulation of this initial grid was already relative fine to ensure a sufficient resolution of all geometric details. The tetrahedral grid however was kept somewhat coarse and was expected to be refined by the adaptation.

This grid was used as initial grid for all symmetric flight conditions and during the simulations it was adapted in four steps for each flight condition. In the adaptation feature of the TAU code the edges of the primary grid are bisected, depending on a refinement sensor. The refinement sensor bases on the differences of the flow variables velocity, density, total pressure and helicity. During the adaptation, points can be added and removed, but only previously added points can be removed. The adaptation algorithm can be started after the computation of a flow solution on a certain grid. It then generates a new grid and interpolates the solution into this grid. The maximum increase of grid points for each of the 4 adaptation loops was limited to 25%. Grid points have been added in the surface grid and in the tetrahedral grid. The new surface points have been included in the prismatic grid, but number and thickness of the prismatic layer have not been changed. (The initial prismatic layer was designed such, that it was suitable for a much finer grid).

With this adaptation procedure the final adapted grid (for example flight condition 25) obtained 1,462,096 surface triangles, 32,375,977 prisms, and 25,871,331 tetrahedra. Compared to the initial grid, these elements roughly have been doubled, resulting in a total number of 21,149,945 nodes. Figure 4-11 shows a comparison of the initial and the final adapted surface grid. New grid points mainly have been added along the leading

edge (leading edge suction), inboard and outboard of the suction peak of the primary vortex (pressure gradient) and in the tip section of the rearward wing. In space, new points have been added in regions with vortical flow above the wing (total pressure, helicity) and in the wake region behind the wing.

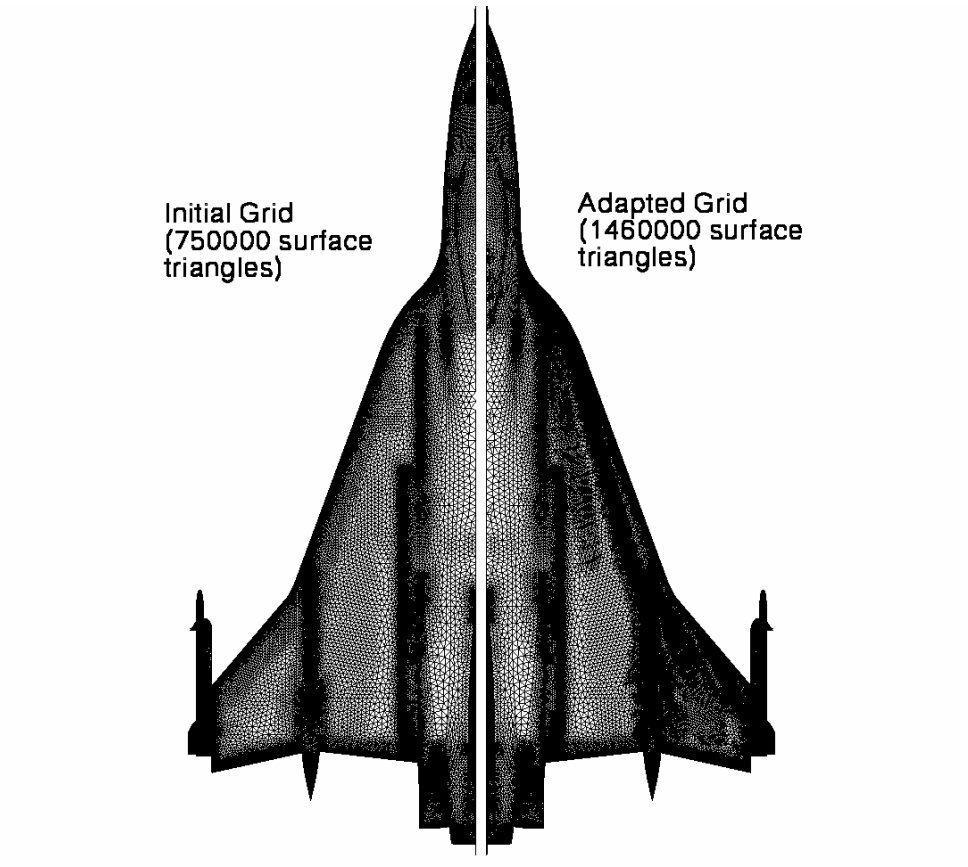

Figure 4-11: Initial EADS-MAS Surface Grid and Final Adapted Grid for Flight Condition 25 (α = 19.84°, M = 0.242).

4.5.2.2 UTSimCenter

One of the more unique grid systems was produced by researchers at the University of Tennessee at Chattanooga Sim Center (UTSimCenter) (see also Chapter 14). Two separate mesh generation programs were used to generate the viscous meshes for these analyses. The first program was a commercially available mesh generation package known as Gridgen [4-13]. Gridgen was used to create an inviscid unstructured mesh. The second mesh generation program was developed in-house at the SimCenter and was used to insert viscous layers in the inviscid mesh.

4.5.2.2.1 Inviscid Mesh

Gridgen was used to create an unstructured inviscid mesh, comprised of mostly tetrahedral [4-13]. Surface meshes, consisting of triangular elements, were created on the geometry defined by the IGES file. Care was

taken to ensure proper resolution of pertinent geometric features such as the leading and trailing edge of the wing. The high curvature of the leading and trailing edges needed fine resolution in the chord-wise direction to resolve the shape. The unstructured triangular surface meshing in Gridgen imposes nearly isometric triangular elements. In order to provide the desired resolution in the chord-wise direction and not have an excessive number of elements in the span wise direction a structured grid was used along the leading and trailing edges of the wing. The aspect ratio of the quadrilateral elements was imposed to be no larger than 15. The resulting structured quadrilateral surface mesh was then converted to an unstructured triangular mesh by subdividing the quadrilateral elements into two triangles. Figure 4-12 shows a section of the leading edge where the converted structured mesh domain meets the unstructured mesh domains. A view of the mesh on the symmetry plane is shown in Figure 4-13.

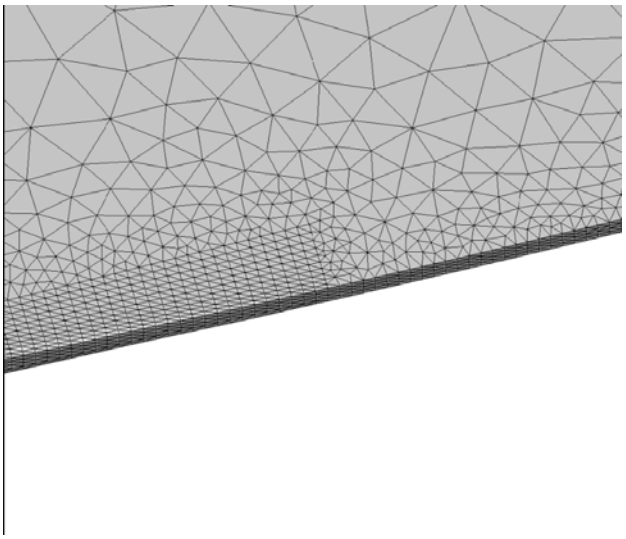

Figure 4-12: Leading Edge Mesh Showing the Converted Structured Mesh Domain Next to an Unstructured Mesh Domain.

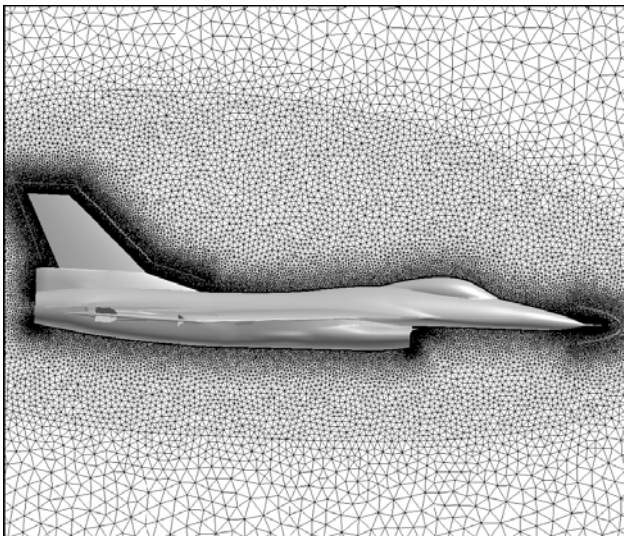

Figure 4-13: Symmetry Plane Mesh.

Baffle surfaces were used to control the spacing of the volume mesh, resulting in a hybrid unstructured inviscid mesh. The quadrilateral elements shown in the figure around the nose and tail are a result of these baffles. Additional baffles were created around the leading edge and trailing edge of the wing and at a near field boundary within a body length of the aircraft.

4.5.2.2.2 Viscous Layer Addition

A second in-house developed mesh generation program was used to insert layers of triangular prismatic elements at the no-slip surfaces of the geometry [4-14]. This method uses a Linear-Elastic mesh-smoothing scheme to push the existing mesh away from the surface, making room for the viscous elements. The term normally used to define Young's Modulus in the Linear-Elastic relations is defined using a combination of element aspect ratio and corner angles to provide stiffness in regions of tight grid spacing. Poisson's ratio was set to a constant of 0.25. Only one layer of points is added at a time in reverse order; the top layer is added first and the final layer near the wall is added last. Points are only added where the local mesh spacing is larger than the desired spacing for the current layer. As a result, the number of triangular prismatic elements in a column varies over the surface. Figure 4-14 and Figure 4-15 show the varying number of elements per

column for the mesh at the inlet. This capability allows the outer layer of prisms to match the spacing of the local tetrahedral elements without forcing each column to have unnecessary layers, which could result in kinking or buckling of the outer viscous layers.

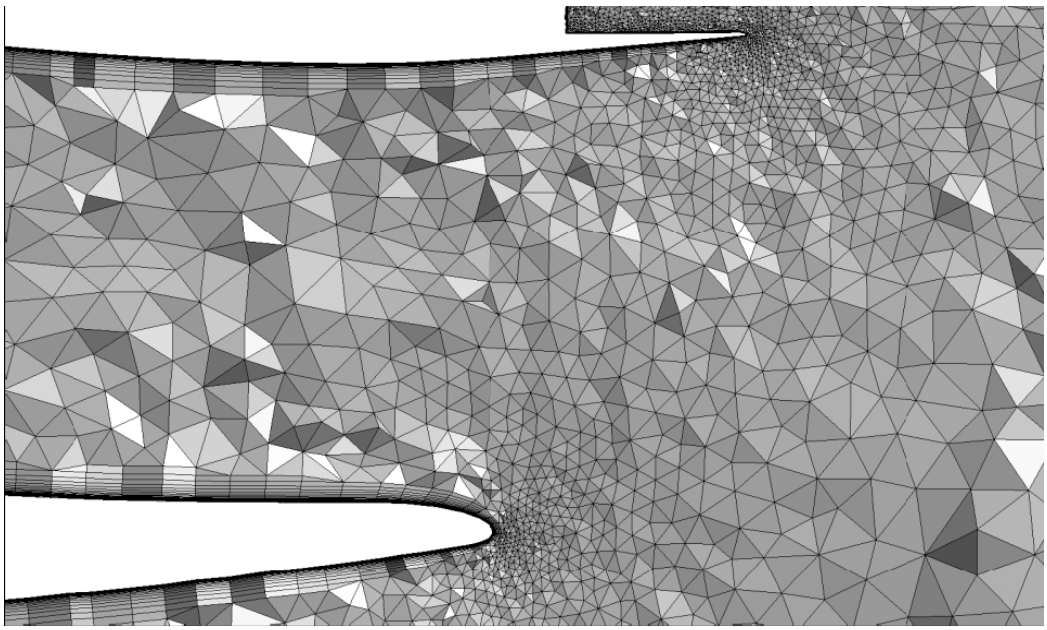

Figure 4-14: Crinkle Cut of Mesh Near the Symmetry Plane at the Inlet.

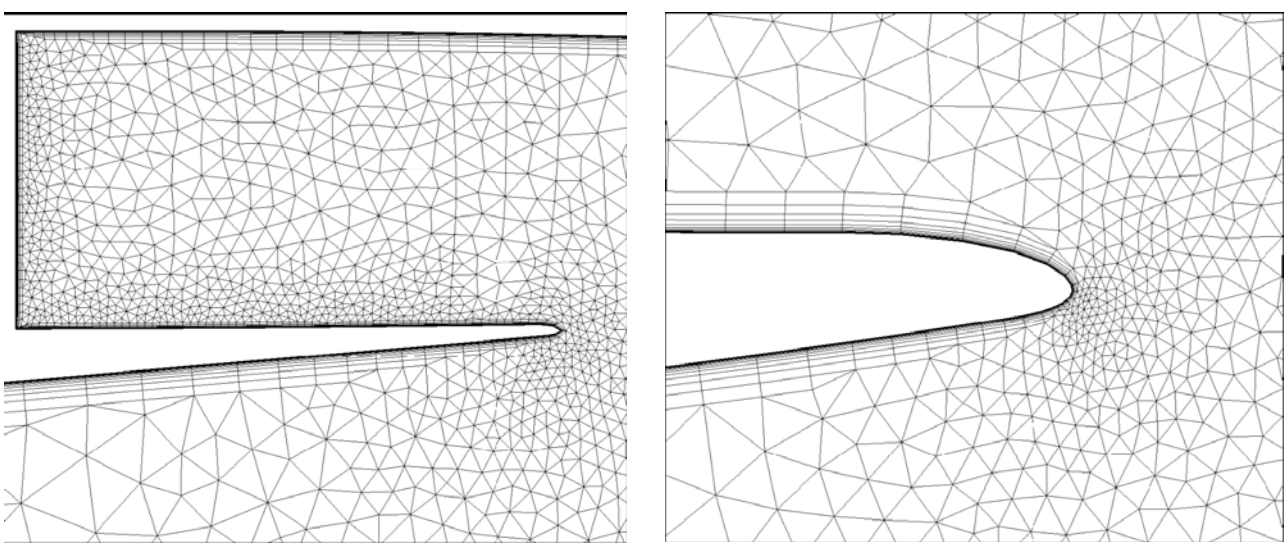

Figure 4-15: Magnified Views of Symmetry Plane Mesh at the Upper Inlet Lip (left) and the Lower Inlet Lip (right).

A total of 25 layers were requested for the viscous region. The initial spacing was specified to correspond to an approximate y^+ value of 1. The height of the subsequent layers increases according to a geometric progression

parameter $\Delta s_2/\Delta s_1$ of 1.15 and a geometric growth rate of 1.02. A view of the viscous layers for the tip missile fins is shown in Figure 4-16. Finer resolution tetrahedra can be seen in the gap region between the fin and the missile rail. The layer insertion strategy matched the normal spacing of the layers with the existing local tetrahedral mesh. The half-model viscous mesh contained 13,906,708 nodes, 32,395,936 tetrahedra, 166,230 pyramid and 15,770,674 prisms.

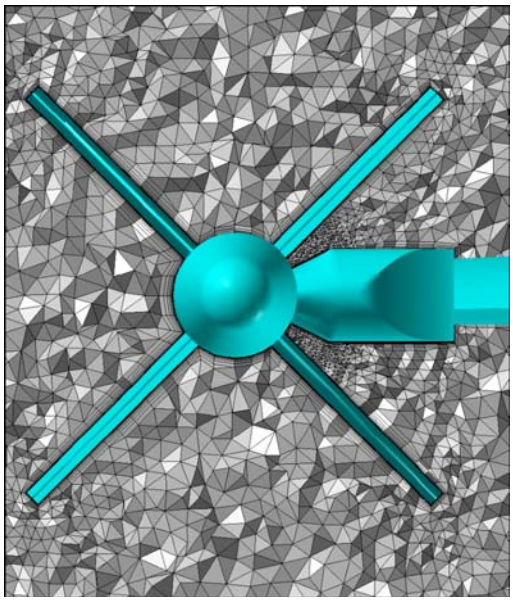

Figure 4-16: Magnified View of Axial Cut Through Tip Missile Fins and Wing.

4.5.2.3 Boeing Phantom Works

The grids used by researchers from the Boeing Phantom Works (see also Chapter 12) were generated using the Boeing Modular Aerodynamic Computational Analysis Process (MADCAP). MADCAP was developed at Boeing as a modular framework to in-house grid generation capabilities from a variety of sources. MADCAP contains a fully automated surface mesh generation capability. In addition to the automated approach, the user can interactively control resolution and mesh element type through the selection of control nodes, edges and surfaces. Unstructured mesh algorithms can be selected from Boeing developed libraries and/or from the Advancing Front with Local Reconnection (AFLR) library [4-15]. Surface meshes can contain a combination of quadrilateral and triangular faces. The volume meshes used in this study were developed with the AFLR code using a combination of element types. Near the wall, advancing layers are used to place highly anisotropic prismatic elements across the boundary layer. Outside the boundary layer, isotropic tetrahedral elements are utilized. A smooth transition between the prismatic and tetrahedral elements is provided by growing each column of the boundary layer mesh until the element at the outside edge is nearly isotropic. The boundary layer resolution is controlled by specification of the initial spacing near the wall, an initial growth rate, a growth stretching and a maximum growth rate. In addition, the extent of the boundary layer thickness can be specified or an estimate of the boundary layer thickness for a turbulent flat plate can be used to extend the prismatic layers beyond the estimate. Control of the resolution of the tetrahedral portion of the mesh is provided by a linear interpolation from the surface mesh. Alternatively, the user can specify a geometry growth rate to control the stretching of resolution in the tetrahedral region. Sources in the form of individual nodes, curves or surfaces can be specified to control the off body resolution of the tetrahedral mesh.

A mesh with higher-resolution than hybrid baseline unstructured grid was constructed in MADCAP to try and improve solution accuracy. In particular, the mesh was concentrated near the wing leading edge to try and improve the prediction near the secondary vortex. Mesh resolution was increased at the leading edge by introducing high aspect ratio quadrilateral elements into the surface mesh. The maximum aspect ratio of the quadrilateral faces is 25. The circumferential resolution at the leading edge is 0.05 inches inboard of the wing crank transitioning to 0.01 inch spacing near the wing tip. The quadrilateral elements were subdivided into triangles in the final mesh. A comparison of the Boeing and common meshes at the wing leading edge is shown in Figure 4-17. The resolution of the Boeing surface mesh is about double that of the common mesh in the immediate proximity of the wing vortices.

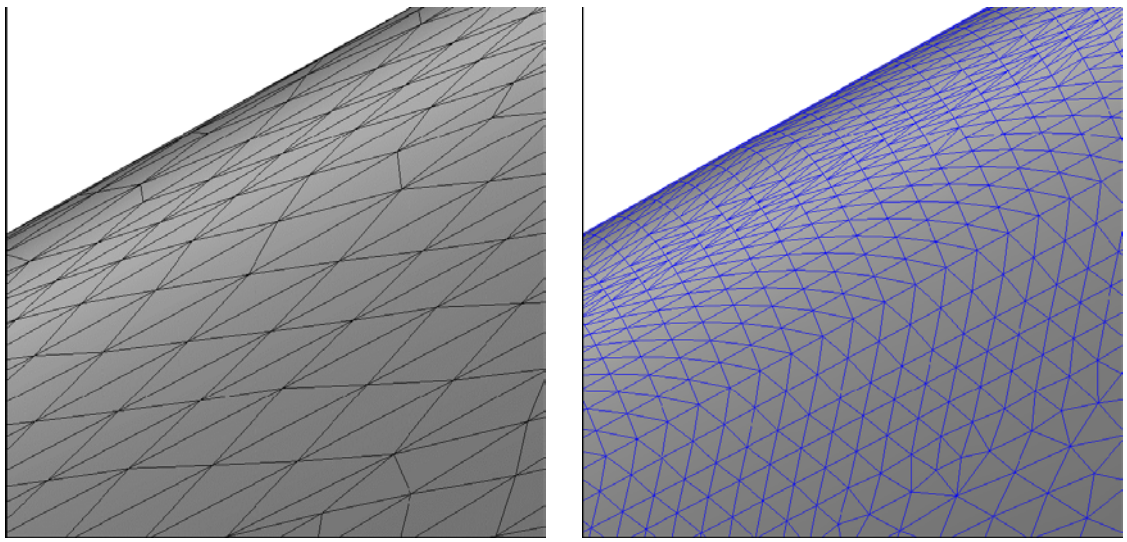

(a) (b)

Figure 4-17: Comparison of Surface Meshes Near the Wing Leading Edge: (a) Hybrid Baseline Unstructured Grid; (b) Boeing Grid.

The volume portion of the Boeing mesh was generated in AFLR and consists of a semi-structured boundary layer extrusion connected to an isotropic tetrahedral grid. The extrusion used a 0.0003 inch initial spacing at the wall to yield a y+ of approximately 1. The initial spacing grew geometrically with an initial geometric progression parameter $\Delta s_2/\Delta s_1$ of 1.2 ending at a 1.8 maximum growth ratio. Extrusion terminated when the prisms achieved an aspect ratio near unity. The combination of the initial viscous spacing, growth rate parameters, and surface spacing produced approximately 15 prism layers. The resulting volume grid had 19.3 million cells.

Feature-based grid adaptation has been used to improve the quality of the grid of the Boeing grids (see Chapter 12).

4.6 CONCLUSIONS

In the framework of CAWAPI both structured and unstructured grids have been generated. Prior to the grid generation an IGES file containing the air tight geometry description of the F-16XL aircraft which could be used for both the structured and unstructured grid generation was created.

The baseline structured grid was generated by NLR using in-house developed (semi-automatic) grid generation algorithms. A family of grids including grids with a reduced number of blocks have been derived from this baseline grid. Although most of the algorithms used had become available just before CAWAPI and thus only a limited experience with their application to such a complex configuration as the F-16XL was available, a grid of good quality was generated within a reasonable amount of time. The best practices established during CAWAPI have resulted in a significant reduction of the grid generation time for future projects.

Several unstructured grids have been generated within CAWAPI. The baseline all-tetrahedral and hybrid unstructured grids were generated at NASA Langley Research Center and the U.S. Air Force Academy, respectively. Despite their rather moderate cell count, the baseline all-tetrahedral and hybrid unstructured grids provided sufficient geometrical resolution. However, several CAWAPI members needed grids with more geometrical resolution. Additional unstructured grids were generated at EADS-MAS, the UTSimCenter, and Boeing Phantom Works.

4.7 ACKNOWLEDGEMENTS

The authors gratefully acknowledges the support provided by Lockheed Martin Aeronautics Company – Fort Worth in providing a refined iges geometry file. In addition, the authors gratefully acknowledges the geometrical work performed by Mr. Edward B. Parlette of Vigyan, Inc. in generating unstructured grids from the iges file.

4.8 REFERENCES

[4-1] Lamar, J.E., Obara, C.J., Fisher, B.D. and Fisher, D.F.: *Flight, Wind-Tunnel, and Computational Fluid Dynamics Comparison for Cranked Arrow Wing (F-16XL-1) at Subsonic and Transonic Speeds*, NASA TP-2001-210629, 2001.

[4-2] *ENFLOW: A Computer Code System for Accurate Simulation of Three-Dimensional Flows*, URL: http://www.nlr.nl/documents/flyers/f222-01.pdf [cited 12 December 2006].

[4-3] Spekreijse, S.P., Prananta, B.B. and Kok, J.C.: *A Simple, Robust and Fast Algorithm to Compute Deformations of Multi-Block Structured Grids*, NLR-TP-2002-105, 2002.

[4-4] Samareh, S.: *GridTool: A Surface Modeling and Grid Generation Tool*, In Proceedings of the Workshop on "Surface Modeling, Grid Generation, and Related Issues in CFD Solutions", NASA CP-3291, May 9-11, 1995.

[4-5] Pirzadeh, S.: *Progress Toward a User-Oriented Unstructured Viscous Grid Generator*, AIAA-96-0031, 1996.

[4-6] Strang, W.Z., Tomaro, R.F. and Grismer, M.J.: *The Defining Methods of Cobalt: A Parallel, Implicit, Unstructured Euler/Navier-Stokes Flow Solver*, AIAA-99-0786, 1999.

[4-7] Wallin, S.: *Standardized Data Format, The Aeronautical Research Institute of Sweden (FFA)*, FFAP-A-950, Stockholm, Sweden, 1992.

[4-8] Eliasson, P.: *EDGE, a Navier-Stokes Solver for Unstructured Grids*, Proc. To Finite Volumes for Complex Applications III, ISBN 1 9039 9634 1, pp. 527-534, 2002.

[4-9] Legensky, S.M., Edwards, D.E., Bush, R.H., Poirier, D.M.A., Rumsey, C.L., Cosner, R.R. and Towne, C.E.: *CFD General Notation System (CGNS): Status and Future Directions*, AIAA-2002-0752, 2002.

[4-10] Lamar, J.E., Cronin, C.K. and Scott, L.E.: *A Review of Steps Taken to Create an International Virtual Laboratory at NASA Langley for Aerodynamic Prediction and Comparison*, Progress in Aerospace Sciences, Vol. 40, No. 3, pp. 163-172, April, 2004.

[4-11] Gerhold, T., Friedrich, O., Evans, J. and Galle, M.: *Calculation of Complex Three-Dimensional Configurations Employing the DLR-Tau Code*, AIAA-97-0167, 1997.

[4-12] CentaurSoft Grid Generator, http://www.centaursoft.com [cited 19 DMarch 2007].

[4-13] Pointwise, Inc., Gridgen User Manual, Version 15, http://www.pointwise.com/ [cited 19 DMarch 2007].

[4-14] Karman, S. Jr.: *Unstructured Viscous Layer Insertion Using Linear-Elastic Smoothing*, AIAA Journal, Vol. 45, No. 1, pp. 168-180, January 2007.

[4-15] Marcum, D.L.: *Advancing-Front/Local-Reconnection (AFLR) Unstructured Grid Generation,* Computational Fluid Dynamics Review, World Scientific – Singapore, 1998, p. 140.

[4-16] TranscenData, http://www.transcendata.com [cited 19 DMarch 2007].